

AD-A114 278

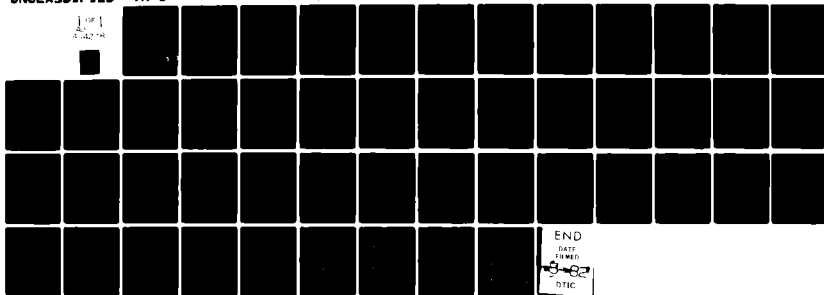
CALIFORNIA UNIV SANTA BARBARA DEPT OF CHEMISTRY F/S 7/4
THE USE OF A PERFECTLY CONDUCTING SPHERE TO EXCITE THE PLASMON --ETC(U)
APR 82 P K ARAVIND; H METIU N00014-A1-K-0598

UNCLASSIFIED

TR-3

NL

1 OF 1
AD-A114 278



END

DATE

FORMED

5-82

DTIC

12

OFFICE OF NAVAL RESEARCH

Contract N00014-81-K-0598

Task No. NR 056-766/4-21-81 (472)

Technical Report No. 3

DA 1142

THE USE OF A PERFECTLY CONDUCTING SPHERE TO EXCITE THE
PLASMON OF A FLAT SURFACE. I. CALCULATION OF THE LOCAL
FIELD WITH APPLICATIONS TO SURFACE ENHANCED SPECTROSCOPY

by

P. K. Aravind and Horia Metiu^(a)

Prepared for Publication

in

Journal of Physical Chemistry

University of California
Department of Chemistry
Santa Barbara, CA 93106

April 1982

Reproduction in whole or in part is permitted for
any purpose of the United States government.

This document has been approved for public release
and sale; its distribution is unlimited.

(a) A. P. Sloan Fellow and Camille and Henry Dreyfus Teacher-Scholar

DTIC
ELECTE
MAY 10 1982

DTIC FILE COPY

80 21 2 112

REPORT DOCUMENTATION PAGE		READ INSTRUCTIONS BEFORE COMPLETING FORM
1. REPORT NUMBER 3	2. GOVT ACCESSION NO. AD-7114-57	3. RECIPIENT'S CATALOG NUMBER 18
4. TITLE (and Subtitle) THE USE OF A PERFECTLY CONDUCTING SPHERE TO EXCITE THE PLASMON OF A FLAT SURFACE. I. CALCU- LATION OF THE LOCAL FIELD WITH APPLICATIONS TO SURFACE ENHANCED SPECTROSCOPY		5. TYPE OF REPORT & PERIOD COVERED Interim Rechnical Report
7. AUTHOR(s) P. K. Aravind and <u>Horia Metiu</u>		6. PERFORMING ORG. REPORT NUMBER
9. PERFORMING ORGANIZATION NAME AND ADDRESS University of California Department of Chemistry Santa Barbara, CA 93106		8. CONTRACT OR GRANT NUMBER(s) N00014-81-K-0598
11. CONTROLLING OFFICE NAME AND ADDRESS Office of Naval Research Department of the Navy, Code: 613A:MAC		10. PROGRAM ELEMENT, PROJECT, TASK AREA & WORK UNIT NUMBERS NR 056-766/4-21-81 (472)
14. MONITORING AGENCY NAME & ADDRESS (if different from Controlling Office)		12. REPORT DATE April 1982
		13. NUMBER OF PAGES 47
		15. SECURITY CLASS. (of this report) unclassified
		15a. DECLASSIFICATION/DOWNGRADING SCHEDULE
16. DISTRIBUTION STATEMENT (of this Report) This document has been approved for public release and sale; its distribution is unlimited.		
17. DISTRIBUTION STATEMENT (of the abstract entered in Block 20, if different from Report)		
18. SUPPLEMENTARY NOTES Prepared for publication in Journal of Physical Chemistry		
19. KEY WORDS (Continue on reverse side if necessary and identify by block number) Surface enhanced spectroscopy. Raman scattering. Electromagnetic theory.		
20. ABSTRACT (Continue on reverse side if necessary and identify by block number) We study the electromagnetic properties of a system consisting of a per- fectly conducting sphere and a dielectric half-space driven by a laser. We show that the local field in the space between the sphere and the plane is strongly enhanced, making the system an interesting candidate for surface enhanced spectroscopy. The dependence of the local field on the incident frequency and the spatial distribution of the enhancement factor are presented. Possible applications are discussed. *		

The use of a perfectly conducting sphere to excite the plasmon of a flat surface. I. Calculation of the local field with applications to surface enhanced spectroscopy.

P.K. Aravind and Horia Metiu^(a)

Department of Chemistry

University of California

Santa Barbara, CA. 93106.



Accession For	
NTIS GRA&I	<input checked="checked" type="checkbox"/>
DTIC TAB	<input type="checkbox"/>
Unannounced	<input type="checkbox"/>
Justification	
By	
Distribution/	
Availability Codes	
Dist	Avail and/or Special
A	

(a) A.P. Sloan Fellow and Camille and Henry Dreyfus Teacher-Scholar.

I. Introduction.

Recent work^[1-10] in a variety of areas of surface spectroscopy indicates that it is possible to modify in a radical manner the spectroscopic signals of a molecule by placing it near a solid surface.

Such modifications can be caused by three electromagnetic effects.

(1) The surface is polarized by the incident beam and the molecule interacts with both the incident and the polarization field. The local light intensity is thus higher and the probability of a molecular excitation is enhanced.

On a flat surface this mechanism produces, at best, a "minor enhancement"^[2] similar to that obtained by placing the molecule near a mirror (whose quality depends on the solid material and the frequency of the incident light). For curved surfaces, however, the light can excite an electromagnetic resonance^[f,g] in the solid which has a strong evanescent field near the surface. This causes a substantial enhancement of the local intensity and of the probability of molecular excitation. Furthermore, the curvature of the surface enhances the field even in the absence of a resonance.

(2) The same mirror effect can produce a minor enhancement^[2] of the emission from an excited molecule. The process is more interesting, however, if the molecular emission frequency coincides with that of an electromagnetic resonance of the surface. The oscillating dipole, representing the emitting molecule, can drive and excite the resonance. The spectroscopic outcome of this depends on whether the resonance prefers to radiate or to use its energy to heat up the surface. If the former is the case the total emission is substantially brighter.

(3) The spectroscopic properties of the molecule are also affected by the molecule-surface energy transfer. This diminishes the lifetime of the molecule and it is thus an "undesirable" effect, unless fluorescence quenching is of interest. Mathematically the rate of transfer is related to the "image

field" of the molecular dipole near the surface, [2, 10] which takes into account the fact that the dipole polarizes the surface and oscillates under the influence of the polarization field. [1g] In doing so it must use a part of its power to sustain the polarization of the solid and this is taken from the power that would have been radiated if the molecule was in vacuum.

It is likely [1f, 1g] that other effects (i.e. "molecular" effects, related to chemisorption) are also at work in surface enhanced spectroscopy. However, we concentrate here on the role of the electromagnetic effects. These are controlled by a number of important factors.

(a) The shape of the surface determines the frequency of the resonance and the magnitude of the evanescent (i.e. near) field. This can be excited by using an ATR (Attenuated Total Reflection) configuration, [3] gratings, [4] spheres and ellipsoids, [5] metal islands, [5c] two spheres, [6] small random roughness [7] and a "coarse" rough surface. [8]

(b) High evanescent fields can be sustained only by materials which are unable to damp the electromagnetic resonance. The ones found useful so far are Au and Cu (~red), Ag (blue and UV), SiC and InSb (infrared).

One of the recent directions taken in this area is a search for new surface geometries, which can permit higher enhancement factors, greater frequency tunability and can function with a broader range of materials. From the point of view of the theorist one would prefer systems which can be prepared in the laboratory and also permit an accurate computation of the electromagnetic effects. In such cases the difference between the experimental observations and the predictions of the electromagnetic model, if any, can be attributed to "molecular" effects.

In what follows we propose such a geometry. This consists of a perfectly conducting sphere "suspended" above a flat surface which has an arbitrary dielectric constant. This system can be prepared^[9] by directing on the flat surface, in a vacuum system, a molecular beam of microscopic metal spheres (radius $\sim 300 \text{ \AA}$ or less) in a carrier gas, and a beam containing the molecules on which one would like to do enhanced spectroscopy. The temperature should be adjusted so that the molecules of interest will freeze on the surface, forming a matrix which traps the metallic spheres. Thus we obtain a flat surface, covered by a molecular matrix containing perfectly conducting spheres. This structure can be prepared for a variety of purposes. One might use a carrier gas which adsorbs on the surface of the spheres and trap the spheres in a spectroscopically inert matrix, on a flat surface that can provide the enhancement; in such a configuration we can study the spectroscopic properties of the molecules adsorbed on the spheres. Another possibility is to preadsorb molecules on the flat surface and then use spectroscopically inert carrier gas to form a matrix which entraps the spheres near the flat surface. This can be used to study the spectra of the molecules adsorbed on the flat surface.

The mechanism for enhancement in this geometry can be qualitatively understood by the description of the following sequence of events. Assume first that the sphere is absent. The laser field cannot excite the surface plasmon of the flat interface because, if it were to do so it would violate parallel momentum conservation.^[1g] The presence of the sphere breaks the translational symmetry along the surface and parallel momentum conservation ceases to be a kinematic requirement. The plasmon can now be excited. The mechanism of this excitation can be understood in the following manner.

The incident light polarizes the sphere and, for large sphere surface distances, the polarization field acting on the surface is that of a dipole. This is known^[10] to excite the plasmon. If the sphere is brought closer to the surface, it is polarized by both the incident laser field and by its own image field. The latter is spatially inhomogeneous and can excite the quadrupole in the sphere, which in turn can also excite the plasmon. The plasmon interacts with the dipole and the quadrupole and its frequency is shifted. Thus the properties of the resonances of this structure are different from those of the plasmon in the absence of the sphere. If the sphere moves closer to the surface the octupole, etc. also play a role. The outcome is that the excited plasmon interacts with the polarized sphere and builds "new" surface resonances which enhance the electric field between the sphere and the surface and whose excitation frequencies are very different from those of the surface plasmon. This large local field can be used to carry out surface enhanced spectroscopy.

The calculation of the local field is rather straightforward in the limit when the distances involved (the radius of the sphere and the plane-sphere separation) are much smaller than the wavelength of light. When this is the case retardation can be neglected and the scalar potential can be calculated by solving Laplace's equation. The solution is obtained by using bispherical coordinates and the method of separation of variables, as exemplified for many cases in the book of Morse and Feshbach.^[11]

The remainder of the paper is organized as follows. In the next section we specify the geometry and outline the procedure used to solve the Laplace equation. Section III presents numerical results chosen to illustrate the properties of the electromagnetic resonances of this particular structure. In the last section we comment on possible applications and compare this system to other candidates for surface enhanced spectroscopy.

II The Model

II.a. The geometry and the materials

The geometry considered here is shown in Fig. 1. It consists of two half-spaces separated by a planar surface. The "optically active" half-space 1, of dielectric constant $\epsilon_1(\omega)$, can sustain a surface excitation (i.e. $\text{Re } \epsilon(\omega)$ can become negative in some frequency range), such as a surface plasmon, polariton or exciton. The other half-space, in which the sphere is imbedded, is "optically inert": its dielectric constant ϵ_0 is real and frequency independent. The sphere is located inside the inert medium at a distance D from the flat surface. It has a large dielectric constant (i.e. good conductor) and its radius is R_0 .

This structure is driven by an external electromagnetic field of frequency ω . The wave vector \vec{k} is contained in the x-z plane and makes an angle θ_0 with the normal to the surface (i.e. the z-axis). To describe the polarization we use the nomenclature associated with flat interfaces: the p-polarized beam has the electric vector in the plane of incidence; the s-polarized beam has the electric vector perpendicular to the plane of incidence (parallel to the surface).

II.b. The method of solution of the Laplace Equation.

We compute the fields in the inert medium for the case when R_0 and D are smaller than the wavelength $2\pi c/\omega$ (Rayleigh limit). In this case we need only to solve the Laplace equation $\nabla^2 \Phi = 0$ for the scalar potential.

The expression for the potential is chosen to be of the form:

$$\Phi = \Phi^{\text{ext}} + \Phi^f + \Phi^s. \quad (1)$$

Here Φ^{ext} corresponds to the laser field and Φ^f to the (Fresnel) field reflected by the flat surface. Φ^s is unknown and takes into account the modifications introduced by the presence of the sphere.

The external field (specified in Fig. 1) is given by

$$\Phi^{\text{ext}}(\vec{r}) = -\vec{E}^i \cdot \vec{r} e^{-i\omega t} \quad (2)$$

The amplitude \vec{E}^i of the electric field is taken to be independent of the spatial coordinate since this is roughly true over the region of interest (around the sphere). We have

$$E_x^i = E_z^i = 0; \quad E_y^i = E_0 \quad (3)$$

(for s-polarization)

and

$$E_x^i = -E_0 \cos \theta_0, \quad E_z^i = E_0 \sin \theta_0, \quad E_y^i = 0, \quad (4)$$

(for p-polarization),

where E_0 is independent of the spatial coordinates.

The potential Φ^f , caused by the presence of the flat surface, is chosen to yield the electric field given by Fresnel formulae. [12]

$$\Phi^f = -\vec{E}^r \cdot \vec{r}, \quad \text{for } z > 0, \quad (5)$$

and

$$\Phi^f = -\vec{E}^t \cdot \vec{r}, \quad \text{for } z < 0. \quad (6)$$

Since only the reflected amplitude \vec{E}^r appears explicitly in the present calculation we reproduce the formulae here. For s-polarized light:

$$E_x^r = E_z^r = 0$$

and

$$E_y^r = E_0 (\cos \theta_0 - \alpha) (\cos \theta_0 + \alpha)^{-1} \equiv E_0 r_s \quad (7)$$

with

$$\alpha = \left\{ (\epsilon_1 / \epsilon_0) - \sin^2 \theta_0 \right\}^{1/2}$$

For p-polarized light:

$$\begin{aligned} E_x^r &= E_0 \cos \theta_0 \left\{ (\epsilon_1 / \epsilon_0) \cos \theta_0 - \alpha \right\} \left\{ (\epsilon_1 / \epsilon_0) \cos \theta_0 + \alpha \right\}^{-1} \equiv \\ &\equiv E_0 \cos \theta_0 r_p, \end{aligned} \quad (8)$$

$$E_z^r = E_x^r \tan \theta_0,$$

and

$$E_y^r = 0.$$

The transmitted field \vec{E}^t is also given by Fresnel formulae,^[12] and we need it when we impose the boundary conditions.

The presence of the sphere affects the total field and these modifications are described by Φ^s . To write an adequate form for the unknown Φ^s we use the bispherical coordinates^[11] μ, η, φ . The x-y plane (i.e. the flat surface) was chosen to coincide with $\mu = 0$, while the surface of the sphere coincides with $\mu = \mu_0$ ($\mu_0 > 0$). The values of μ_0 and the scale factor c_0 are determined by R_0 and D through

$$\mu_0 = \operatorname{arccosh} (1 + D/R_0) = \ln \left\{ [1 + (D/R_0)] + [2(D/R_0) + (D/R_0)^2]^{1/2} \right\} \quad (9)$$

$$c_0 = R_0 \left\{ (1 + D/R_0)^2 - 1 \right\}^{1/2} \quad (10)$$

The expression for Φ^s in the inert medium ($0 < \mu < \mu_0$) has the form

$$\Phi^s(\mu, \eta, \varphi) = F \sum_{n \geq |m|}^{\infty} \sum_{m=-\infty}^{+\infty} \left\{ A_n^m \exp[(n+1/2)\mu] + B_n^m \exp[-(n+1/2)\mu] \right\} Y_n^m(\cos \eta, \varphi). \quad (11)$$

Inside the active medium ($\mu < 0$) we write:

$$\Phi^s(\mu, \eta, \varphi) = F \sum_{n \geq |m|}^{\infty} \sum_{m=-\infty}^{+\infty} D_n^m \exp[(n+1/2)\mu] Y_n^m(\cos \eta, \varphi) \quad (12)$$

The definition used for the spherical harmonics Y_n^m is that of Morse and Feshbach^[11] and $F = (\cosh \mu - \cos \eta)^{1/2}$.

We have chosen these functional forms for the potentials because they are general solutions of the Laplace equation with the correct behaviour at infinity. The unknown coefficients A_n^m , B_n^m and D_n^m are determined by imposing the boundary conditions

$$\Phi(\mu = 0^+, \eta, \varphi) = \Phi(\mu = 0^-, \eta, \varphi), \quad (13)$$

$$\epsilon_0 \frac{\partial \Phi}{\partial \mu} (\mu = 0^+, \eta, \varphi) = \epsilon_1(\omega) \frac{\partial \Phi}{\partial \mu} (\mu = 0^-, \eta, \varphi) \quad (14)$$

and

$$\Phi(\mu_0, \eta, \varphi) = V_0. \quad (15)$$

The first two match the potential and its derivative at the flat interface. The inert half space is at $\mu = 0^+$ and the active one at $\mu = 0^-$. The third condition recognizes the fact that the field inside the perfectly conducting sphere is zero and that the surface of the sphere is a surface of equal potential V_0 . The potential V_0 is determined from the requirement that the total charge on the surface of the sphere is zero.

II.c. The results for Φ

Implementing this procedure yields the following results for the coefficients A_n^m , B_n^m and D_n^m .

For s-polarized light

$$A_n^m = B_n^m = D_n^m = 0 \quad \text{if } m \neq \pm 1 \quad (16)$$

$$A_n^1 = A_n^{-1} = i(1+r_s)c_o E_o \sqrt{2} \left\{ \exp[(2n+1)\mu_o] + \mathcal{X}_1 \right\}^{-1} \cdot \left\{ 4\pi n(n+1)/(2n+1) \right\}^{1/2}. \quad (17)$$

with

$$\mathcal{X}_1 = [\epsilon_o - \epsilon_1(\omega)] [\epsilon_o + \epsilon_1(\omega)]^{-1}. \quad (18)$$

Furthermore

$$B_n^{\pm 1} = \mathcal{X}_1 A_n^{\pm 1} \quad (19)$$

and

$$D_n^{\pm 1} = (1 + \mathcal{X}_1) A_n^{\pm 1}. \quad (20)$$

For p-polarized light we obtain

$$A_n^0 = [4\pi/(2n+1)]^{1/2} \left\{ \sqrt{2} V_o + c_o E_o \sqrt{2} (1+r_p)(2n+1) \sin \theta_o \right\} \cdot \left\{ \exp[(2n+1)\mu_o] + \mathcal{X}_1 \right\}^{-1}, \quad (21)$$

$$A_n^1 = -A_n^{-1} = \sqrt{2} c_o E_o [4\pi n(n+1)/(2n+1)]^{1/2} (1-r_p) \cos \theta_o \cdot \left\{ \exp[(2n+1)\mu_o] + \mathcal{X}_1 \right\}^{-1}, \quad (22)$$

$$B_n^{0, \pm 1} = \mathcal{X}_1 A_n^{0, \pm 1}, \quad (23)$$

$$D_n^{0, \pm 1} = (1 + \mathcal{X}_1) A_n^{0, \pm 1}, \quad (24)$$

and

$$A_n^m = B_n^m = D_n^m = 0 \text{ if } m \neq 0, \pm 1 \quad (25)$$

The quantity V_0 is

$$V_0 = -c_0 E_0 (1 + r_p) \sin \theta_0 \left. \frac{\partial}{\partial \alpha} \ln \sum_{n=0}^{\infty} \alpha^{2n+1} [\exp((2n+1)\mu_0) + \chi_1]^{-1} \right|_{\alpha=1} \quad (26)$$

II.d. The resonances of the structure.

An examination of the equations giving the coefficients A_n^m , B_n^m , and D_n^m , for both s- or p-polarized light, shows that the potential Φ^s might have special properties (both inside and outside of medium 1) at frequencies ω_n satisfying

$$\exp[(2n+1)\mu_0] = -\operatorname{Re} \chi_1(\omega_n) = \operatorname{Re} \left(\frac{\epsilon(\omega_n) - 1}{\epsilon(\omega_n) + 1} \right); n = 0, 1, 2, \dots \quad (27)$$

When this condition is fulfilled the quantity $\{\exp[(2n+1)\mu_0] + \chi_1(\omega)\}^{-1}$, appearing in the coefficients A_n^m , B_n^m , and D_n^m , takes its largest value, $\{\operatorname{Im} \chi_1(\omega_n)\}^{-1}$. If $\operatorname{Im} \chi_1(\omega_n)$ is small, the potential Φ^s can be substantially enhanced at the frequencies ω_n .

It is instructive to examine the frequencies ω_n for the case when the dielectric constant of the active medium is given by a Drude model lacking dissipation,^[14] for which $\epsilon_1(\omega) = 1 - (\omega_p/\omega)^2$. Here ω_p is the plasmon frequency. For this simple case Eq. (27) gives

$$\omega_n = \frac{\omega_p}{\sqrt{2}} \left\{ 1 - \exp[(2n+1)\mu_0] \right\}^{1/2}. \quad (28)$$

If $(2n+1)\mu_0 \gg 1$ the resonance frequency $\omega_n \rightarrow \omega_p/\sqrt{2}$ which is the frequency of the surface plasmon. However, in the other extreme, when $(2n+1)\mu_0$ is very small, the resonance frequencies are

$$\omega_n = \frac{\omega_p}{\sqrt{2}} \left\{ (2n+1)\mu_0 \right\}^{1/2} \quad (29)$$

The lowest resonance frequency, for low $(2n+1)\mu_0$, is at $\omega_{n=0} = (\omega_p/\sqrt{2})\sqrt{\mu_0}$. From Eq. (9) we see that this limiting case appears when $\lambda \equiv D/R_0 \ll 1$ and gives the lowest frequency $\omega_{n=0} = \omega_p(\lambda/2)^{1/2}$. If the sphere touches the surface, $\omega_{n=0} \rightarrow 0$.

For real materials the analysis is more complicated and depends on the dielectric constant $\epsilon_1(\omega)$ of the material and the properties of its surface resonance. A discussion of a few practical cases can be found in Section III. We show there that even though the coefficients A_n^m , B_n^m and D_n^m are maximized when $\omega = \omega_n$, this does not necessarily lead to an enhanced value of the potential.

II.e. The electric fields and the local intensity.

The electric field in the space occupied by the inert medium is computed from

$$E_i = - \frac{1}{h_i} \frac{\partial \Phi}{\partial i}, \quad i = \mu, \eta, \varphi, \quad 0 < \mu < \mu_0. \quad (30)$$

with^[11] $h_\mu = h_\eta = c_0 [\cosh \mu - \cos \eta]^{-1}$ and $h_\varphi = c_0 \sin \eta [\cosh \mu - \cos \eta]^{-1}$.

If we place an isotropic molecule in this field, a dipole $\vec{p}(\omega) = \alpha \vec{E}(\omega)$ is induced and this leads to a spectroscopic signal from the molecule.

In most cases the intensity measured in a spectroscopic experiment is proportional to $\vec{p}(\omega) \cdot \vec{p}(\omega)^* \sim \alpha \alpha^* \vec{E}(\omega) \cdot \vec{E}^*(\omega)$. The quantity $\vec{E} \cdot \vec{E}^*$ is thus a key electromagnetic quantity. Since we have many parameters (such as ω , θ_0 , the polarization, the point where the field is calculated, D/R_0 , ϵ_1 and ϵ_0) we prefer to plot this "local field intensity":

$$I = E_{\mu} E_{\mu}^* + E_{\eta} E_{\eta}^* + E_{\varphi} E_{\varphi}^* \quad (31)$$

rather than give information concerning the direction of \vec{E} , which is not qualitatively important for our present purposes.

II.f. The approximations involved.

The use of an electrostatic calculation involves certain approximations which we want to state explicitly.

(1) The use of the Laplace equation to compute the electric field is normally justified if the linear dimensions of the solid are smaller than the wavelength of the incident light. In our case the flat interface between the inert and the active media does not satisfy such a requirement. For this reason we have used the equation (1) which contains explicitly (through Φ^f) the exact solution of Maxwell's equations, for the case when the sphere is absent. We use an electrostatic (Rayleigh) approximation only for the computation of Φ^s . This is the potential caused by the presence of the sphere. It contains the effect of the polarization of the sphere and ^{the} "image field" induced by the polarization of the sphere. The latter is necessary because the flat surface is present. This polarization is confined to a region whose linear extent is of the order $2(2R_0 + D)$. When this is smaller than $2\pi c/\omega$ we expect the electrostatic approximation to hold.

(2) The assumption that the radiation caused by the polarization of a region of size $2(2R_0 + D) \ll 2\pi c/\omega$ is that corresponding to the dipole induced in that region can be justified rigorously.^[13] The scattering due to the planar interface is treated here exactly by using Fresnel formulae for Φ^f .

(3) It is well known^[12] that the magnetic dipole of a perfectly conducting sphere makes an important contribution to the intensity of the light scattered by such an object. The electrostatic calculation carried out by us eliminates this effect. Fortunately, the magnetic dipole effects are important in the radiation zone only, and contribute negligibly to the near field computed here.

III. The results of the numerical calculations.

III.1. Objectives.

The electromagnetic properties of the structure considered here depend on a large number of parameters. To diminish the amount of interesting-but-not-essential information we plot only the "enhancement ratio"

$$\tilde{I} = (\mathbf{E}_\mu \mathbf{E}_\mu^* + \mathbf{E}_\eta \mathbf{E}_\eta^* + \mathbf{E}_\phi \mathbf{E}_\phi^*) / \mathbf{E}_0 \cdot \mathbf{E}_0^*, \quad (32)$$

which is the ratio of the local and the incident intensity. The graphs presented in what follows have the following objectives.

- (1) We want to study the frequency dependence of \tilde{I} in order to learn the resonance frequencies, and the width and magnitude of the resonant enhancement. By varying the geometrical parameters (i.e. $\lambda = D/R_0$) and nature of the active material we want to exemplify the "tunability" of the structure.
- (2) In analyzing the explicit formulae for the expansion coefficients A_n^m and B_n^m we discuss the origin of the observed resonances and their frequency, and also elucidate their role in giving rise to the observed resonant enhancement.
- (3) Finally, a group of graphs illustrates the spatial properties of the enhancement factor \tilde{I} .

III.2. The materials.

The calculations are valid for systems chosen so that the sphere is a good conductor and its size satisfies the requirements discussed in Section II. There are no limitations on the active materials except, of course, for the fact that we desire large enhancements in a spectroscopically interesting frequency range; this is accomplished if the electromagnetic resonances of the structure that appear in the desirable frequency range are poorly damped.

Silver is by now the best loved enhancer for incident visible (blue and near UV) light. The flat surface has a surface plasmon with the dispersion relation $k_{||} = (\omega/c) \operatorname{Re} \left(\epsilon_1(\omega) / (\epsilon_1(\omega) + 1) \right)$. This cannot be excited by light but it can be excited by any localized source placed near the surface, such as an excited molecule^[10] or a polarized sphere.^[15] Such sources excite the high $k_{||}$ region of the dispersion curve (i.e. the unretarded plasmon) at the frequency given by $\operatorname{Re} \epsilon_1(\omega) = -1$. For silver^[16] this is at $\omega_{sp} = 3.62 \text{ eV}$.

β -Silicon carbide is a newcomer which is an excellent enhancer in infrared. Its dielectric constant is given by^[17]

$$\epsilon(\omega) = \epsilon_{\infty} (\omega_L^2 - \omega^2 - i\omega\gamma) (\omega_T^2 - \omega^2 - i\omega\gamma)^{-1} \quad (33)$$

The parameters appearing in this equation are $\epsilon_{\infty} = 6.7$, $\omega_T = 794 \text{ cm}^{-1}$, (i.e. the restrahl frequency corresponding to maximum reflectivity), $\omega_L = 970 \text{ cm}^{-1}$ and $\gamma = 8.5 \text{ cm}^{-1}$. The surface resonance is a surface polariton. Its high $k_{||}$ (i.e. unretarded) frequency is given by $\epsilon(\omega) = -1$ and equals $\omega_{sp} = 949 \text{ cm}^{-1}$.

InSb is a semi-conductor whose dielectric constant is given by^[18]

$$\epsilon(\omega) = \epsilon_{\infty} + \frac{S\omega_o^2}{\omega_o^2 - \omega^2 - i\omega\gamma} - \frac{\omega_p^2 \epsilon_{\infty}}{\omega^2 + i\omega\omega_c} \quad (34)$$

The parameters are: $\epsilon_{\infty} = 15.7$, $S = 2.2$, $\omega_o = 179 \text{ cm}^{-1}$, $\gamma = 2.7 \text{ cm}^{-1}$, $\omega_p = 1023 \text{ cm}^{-1}$, $\omega_c = 30 \text{ cm}^{-1}$.

The second term in Eq. (34) represents contributions to the dielectric constant caused by optical phonons. The third is due to conduction electrons. A useful feature of n-type InSb is that we can modify the bulk plasmon frequency by doping, since ω_p depends on the free electron density N through $\omega_p = (4\pi Ne^2/m^*\epsilon_\infty)^{1/2}$.

The material has three unretarded surface modes, since there are three frequencies at which $\text{Re } \epsilon(\omega)$ equals -1 . The low frequency mode is mainly a surface polariton and the high frequency one is mainly a surface plasmon. Since the width of the resonance equals $\text{Im } \epsilon(\omega)$ taken at the resonance frequency, only the plasmon like mode is expected to play an important role if high local fields are desired. The other two can, however, be very effective in dissipating the energy of vibrationally excited molecules which resonate with them.

Doping affects the plasmon mode by shifting its frequency to higher values until the maximum frequency $\omega_p [\epsilon_\infty/(\epsilon_\infty+1)]^{1/2} = 992 \text{ cm}^{-1}$ is reached. Through plasmon-polariton "interaction" doping also shifts the frequency of the polariton resonance. The minimum value is ω_0 .

We also consider an "organic material" of the kind studied by Pockrand et.al.^[19] in their ATR work. A representative dielectric constant is

$$\epsilon(\omega) = \epsilon_\infty + \frac{\omega_T^2 f}{\omega_T^2 - \omega^2 - i\omega/\delta}, \quad (35)$$

with $\epsilon_\infty = 2.25$, $f = 0.2$, $\omega_T = 2.24 \text{ eV}$ and $\delta = 22.34 \text{ eV}^{-1}$. The unretarded surface mode is a surface exciton.

III.3. The Frequency dependence of the enhancement factor.

III.3.a. Silver substrate.

In Fig. 2 we plot \tilde{I} , as a function of frequency, for two different values of the geometrical factor $\lambda = D_0/R$. The point at which \tilde{I} is calculated is located on the flat interface directly below the sphere (at $x_0 = z_0 = 0$ in Fig. 1). This point was chosen because the enhancement factor there is very high. The frequency dependence of \tilde{I} (i.e. the shape of the curve) is weakly dependent on the observation point as can be seen from the Eqs. (11) and (16) - (19). The observation point enters in the spherical harmonics and the exponentials $\exp [\pm (n+1/2)\mu]$. The resonant behaviour (i.e., the shape of the frequency dependence curve) enters in A_n^m and B_n^m . A change in observation point can change radically the magnitude of the enhancement but not the resonant structure of the curve (as long as the point is close enough to the sphere). The maximum enhancement is $\tilde{I} = 8300$ (for $\lambda = 0.05$ given, for example, by $R_0 = 100 \text{ \AA}$ and $D = 5 \text{ \AA}$) and it occurs at 3.27 eV. The resonance is very broad. If the sphere is moved further from the flat surface the maximum enhancement is $(6.315) \cdot 10^3$ at frequency 3.43 eV. Note that in the case of Raman scattering the enhancement of the emission is comparable to that of the local field^[20] and therefore if $\tilde{I} \sim 10^3$ the Raman enhancement is $\sim 10^6$.

III.3.b. β -Silicon carbide substrate.

The dependence of \tilde{I} on ω , when the active medium is β -SiC, is displayed in Fig. 3a. For $\lambda=0.1$ (i.e. $R_0 = 100 \text{ \AA}$, $D = 10 \text{ \AA}$) \tilde{I} has a peak value of $\sim 10^4$, located at $\omega = 928 \text{ cm}^{-1}$. For $\lambda=0.05$ (i.e. $R_0 = 100 \text{ \AA}$ and $D = 5 \text{ \AA}$) there are two peaks, at $\omega = 916 \text{ cm}^{-1}$ and 935 cm^{-1} . This happens because the damping of the gap modes is too small to make them merge in a broad peak. This is further discussed in Section III.4.

The s-polarized light is not as efficient in creating large local fields. This is seen in Fig. 3(b), where \tilde{I} is plotted for conditions identical to Fig. 3(a), except for the polarization. The s-polarized light yields an enhancement of ~ 600 , which is about two orders of magnitude lower than that obtained with p-polarized light. This is the result of a symmetry effect which appears because the electric field parallel to the flat surface does not excite modes in which the induced charge oscillates perpendicular to the surface. Mathematically this appears in the equations through the fact that $A_n^m = B_n^m = 0$ for $m \neq \pm 1$ so that the mode $m=0$ is not excited. The p-polarized light excites all the modes, and it excites the $m=0$ mode more strongly as $\theta \rightarrow 90^\circ$. Thus, p-polarized light at grazing incidence is most effective.

We have found previously^[1g] a propensity rule which states that a maximum local field is created between two boundaries if the electric field of the excitation source oscillates along the line uniting the two boundaries. This happens as if the electrons try to follow the field and are pushed against the boundaries causing a charge concentration which increases the field in the vacuum, between the boundaries.

III.3.c. InSb substrate.

The frequency dependence of \tilde{I} , for the case when the active medium is InSb, is presented in Figs. 4(a) and (b). The incident laser characteristics and the geometry of the system are the same as in Fig. 2. The figures differ through the bulk plasmon frequency which is $\omega_p = 195 \text{ cm}^{-1}$, for 4(a), and $\omega_p = 1023 \text{ cm}^{-1}$, for 4(b). Such differences can be achieved through doping. At low conduction electron concentration one can see two sets of gap modes, one at 140 cm^{-1} and the other at 200 cm^{-1} . These bands are composed of several gap modes which have a sizeable width and overlap. The shoulder at 170 cm^{-1} is an indication of the existence of such modes. In Fig. 4b we show the local enhancement factor caused by the surface plasmon in heavily doped InSb. The surface polariton does not give a large local enhancement, probably because of large values of $\text{Im} \chi_1(\omega)$ at that frequency. Note that doping shifts upwards the frequency of the gap mode and increases substantially the enhancement at that frequency.

III.3.d. Organic substrate

We have carried out a calculation with the active medium whose dielectric constant^[19] is typical of organic crystals such as anthracene. The surface mode excited by the sphere to form the gap modes is a surface exciton. The enhancement is modest (Fig. 5) as compared to the other active media considered here, but it is sufficiently large to carry out surface enhanced spectroscopy.

III.4. The frequency of the gap modes and the structure of the resonance spectrum.

In this section we wish to examine more closely the connection between the gap mode frequencies (i.e., the solutions of Eq. (27)) and the overall frequency response of the system. As indicated earlier, the gap mode frequencies are determined by the vanishing of the denominators of the expansion coefficients A_n and B_n . These denominators are of the form $\{\exp[(2n+1)\mu_0] + \chi_1(\omega)\}$, where μ_0 is given by Eq. (9), $\chi_1(\omega) = (1 - \epsilon_1(\omega)(1 + \epsilon_1(\omega))^{-1})$ and $n = 0, 1, 2, \dots$. If we plot $-\text{Re}\chi_1(\omega)$ and $-\text{Im}\chi_1(\omega)$ as functions of ω , the (gap mode) resonance frequencies are located at the intercept of the horizontal lines corresponding to $\exp((2n+1)\mu_0)$ with $-\text{Re}\chi_1(\omega)$. The enhancement for each resonance is inversely proportional to the value of $\text{Im}\chi_1(\omega)$ at its frequency. This is illustrated in Fig. 6 for a SiC substrate. The dotted lines are the magnitudes of $\exp((2n+1)\mu_0)$ for $n = 0, 1, 2$ and 3. For $n = 0$ there are two resonances, one at $\omega_0^{(1)} \approx 888 \text{ cm}^{-1}$ and the other at $\omega_0^{(2)} \approx 949 \text{ cm}^{-1}$. The upper mode $\omega_0^{(2)}$ occurs at practically the same frequency as the surface polariton of the flat substrate, i.e., it is obtainable to good accuracy as the root of the equation $\text{Re}\chi_1(\omega) = 0$ or $\epsilon_1(\omega) = -1$. However, unlike the latter, it is strongly damped (due to the large value of $\text{Im}\chi_1(\omega)$) and is therefore not a well defined excitation of the sphere-plane system. The lower mode $\omega_0^{(1)}$ has a very small damping associated with it and is therefore a well defined excitation of the system. The role of the conducting particle atop the substrate is thus seen to be the following: it strongly damps the original (surface polariton) mode at $\omega_0^{(2)}$ and creates a new (gap-mode) resonance at the appreciably lower frequency $\omega_0^{(1)}$. These features persist for the higher gap modes. For $n = 1, 2$ the gap modes occur at 929 cm^{-1} and

940 cm^{-1} , respectively. For $n \geq 3$, there is no intercept between $-\text{Re}X_1(\omega)$ and $\exp((2n+1)\mu_0)$ and thus there are no well defined gap modes. Another way of saying this is that for $n \geq 3$ the gap modes have been pushed up towards the surface polariton frequency of 949 cm^{-1} where they are strongly damped because of the large value of $\text{Im}X_1(\omega)$.

The foregoing analysis would seem to indicate that of all the gap modes it is only the lowest few (perhaps the first two or three) that are important in determining the response of the system. In fact, in the case under study here, the lowest ($n=0$) mode alone seems to be all important since its damping is more than an order of magnitude smaller than for the higher modes. One might therefore be tempted to conclude that the overall resonant response of the system would be at the frequency of the lowest gap mode ($=388 \text{ cm}^{-1}$) and have a magnitude inversely proportional to the square of $\text{Im}X_1(\omega)$ there. The actual situation turns out to be more complicated than this. The reason is that the relative contribution of the different modes to the potential (and hence to the field intensity) is given by an expression of the form (Eq. (11))

$$\sum_{nm} A_n^m \exp[(n + 1/2)\mu] Y_n^m(\eta, \varphi)$$

In the preceeding analysis we looked only at the coefficients A_n^0 . However, in order to obtain the relative importance of different modes we must compare the quantities $A_n^m e^{(n+1/2)\mu} Y_n^m$ for different n . This is done in Table 1, where we restrict our attention to terms with $m = 0$. In the second column we list the absolute value (modulus) of A_n^0 . As expected, A_n^0 decreases rapidly with increasing n (the frequency at which these calculations have been made is that of the lowest gap mode $= 888 \text{ cm}^{-1}$).

In the 3rd column we show the quantity $e^{(n+1/2)\mu_0}$ and in the 4th the product $e^{(n+1/2)\mu_0} |A_n^0|$ (we disregard here the spherical harmonic Y_n^0 which is generally of order unity). Note that the 4th column decreases much less rapidly with increasing n than the 2nd column. This is because the decrease of $|A_n^0|$ is offset to some extent by the increase of the exponential factor $e^{(n+1/2)\mu_0}$. The 4th column shows clearly that it is not just the lowest mode which is important but a large number of low lying modes; this is evident from the fact that the cumulative effect of modes 1 through 7 is as important as the lowest ($n=0$) mode. For n larger than 10 or so $|A_n^0|$ plunges sharply and so does the product in the last column, thus making the contribution of these modes rapidly less important.

We can conclude from our analysis of the previous paragraph that the overall frequency response of the system is determined by the contribution of a large number of low-lying gap modes, and not just the lowest mode as our preliminary analysis seemed to indicate. The competition between the modes results from the finite damping of the substrate. If the substrate had no damping ($\text{Im } \epsilon_1(\omega) = 0$) there would be an infinite number of gap modes at each of which the response (measured by the local field intensity) would be infinite. With finite damping ($\text{Im } \epsilon_1(\omega) \neq 0$) the modes are broadened and overlap with each other. As a result of this smearing out, the system response peaks at a frequency intermediate between that of the lowest gap mode (888 cm^{-1}) and the upper surface polariton cutoff (949 cm^{-1}) — in the present case this is at 916 cm^{-1} with a secondary peak at 935 cm^{-1} .

III.5. The spatial extent of the enhanced field.

We present now several graphs which display the spatial distribution of the localized enhancement \tilde{I} , when the excitation frequency corresponds to the maximum local field enhancement. We take $\lambda = 0.05$ (i.e. $R_0 = 100 \text{ \AA}$ and $D = 5 \text{ \AA}$), $\theta_0 = 60^\circ$, and p-polarized light. We compute \tilde{I} in the plane of incidence of light, along specific curves. In Figs. 8 we show the variation of \tilde{I} along a circle surrounding the sphere. The distance to the sphere surface is 1 \AA . The variable is the polar angle θ of the observation point. The largest enhancement is obtained for $\theta = \pm 180^\circ$, which corresponds to points located between the sphere and the planar surface. The field has a minimum near $\theta = -90^\circ$, which is located in the "shadow" of the sphere. Larger fields are obtained on the "sunny" side of the structure (i.e. $0 \lesssim \theta \lesssim 90$).

Note that the spatial distribution of the local intensity is very similar for Ag, SiC (Fig. 8(a)), InSb and the organic material (Fig. 8(b)). All these graphs were computed at the resonance frequency of each material. The curves would probably be very different if they were all computed at the same frequency.

In Fig. 9 we show the fields along the symmetry axis of the system, in the space between the sphere and the plane. The enhancement is very high and constant along the line. In Fig. 10 we plot the enhancement factor along the line AB shown in Fig. 1. The local intensity decays as one moves from A towards B. At points approximately 100 \AA away from A, \tilde{I} reaches the small value it would have for a flat surface in the absence of the sphere. The curves are very similar for different active materials as long as the calculation is carried out at the resonance frequency of each material.

IV. Discussion.

The calculations presented here indicate that the gap modes formed between a perfectly conducting sphere and an optically active medium are potentially useful for surface enhanced spectroscopy. The sphere permits the optical excitation of the flat surface mode (surface plasmon, or polariton, or exciton) but it distorts it so strongly that it seems useful to regard these resonances as new modes. The name of gap modes seems appropriate. The local intensity is concentrated between the sphere and the plane, with large contributions at the illuminated side of the sphere and smaller contributions on the shady side. This is very different from a mode of the flat surface which is delocalized along the plane.

The enhancement factor produced by the gap modes is very large, but unfortunately its spatial extent is small. This is not by accident, since one can think of the enhancement process as resulting from trapping a photon in the gap region. Thus the delocalized photon energy is packed in a small volume and, since the field energy per unit volume is proportional to $\vec{E} \cdot \vec{E}$, the conservation of the total energy requires that $\vec{E} \cdot \vec{E}$ be large in the small region. The ability of generating large enhancements is insured by large oscillator strength (so that the number of absorbed photons is large) and the existence of electromagnetic and geometric factors which pack the photon energy in a small space. Our structure seems to satisfy these requirements. However, the number of molecules that can be exposed to high fields goes down. One can try to compensate for this by depositing on the surface a large number of spheres, with the largest radius for which $2R_0 \ll 2\pi c/\omega$. However, one should keep in mind that if the sphere concentration becomes too large the gap modes may interact with each other, become delocalized and thus lower the

enhancement factor. Such effects are very difficult to compute accurately or estimate reliably; it is probably better to study them experimentally.

One can envision several types of applications. (a) Pre-adsorb the molecules of interest on an active single crystal substrate (e.g. Ag, β -SiC, InSb) and deposit on the flat surface chemically inert perfect metal spheres, imbedded in an optically and chemically inert matrix. One can then attempt to use the structure thus obtained to study the spectroscopic properties of the preadsorbed molecules. (b) Assume now that one is interested in the spectroscopic properties of molecules adsorbed on small metal particles. To carry out enhanced IR spectroscopy one can place these particles on a InSb surface after adsorbing on them the molecules of interest. One can hope, by doping InSb, to be able to tune the structure to have a resonance at the molecular frequency of interest. The molecules will absorb very strongly at the molecular frequency and thus depress the resonance. One can hope to detect this effect in several ways: (α) difference spectra, with and without the absorbing molecules: (β) polarization modulation, since the absorption from a p-polarized beam is much stronger than that from a s-polarized beam; (γ) by monitoring the local temperature with a bolometer. We are now in process of carrying out computations to evaluate the chances that such measurements might succeed. (c) The structure can also be used to attempt to carry out infra-red (on InSb and β -SiC) or visible (Ag) multiphoton photochemistry or non-linear spectroscopy. (d) Finally, one can think of making use of the effects described here to construct IR detectors, especially if one is interested in having a detector for a small, given frequency range. One can use an InSb film and metal particles trapped on its surface by a matrix whose molecules absorb in the desired range. By doping the InSb

film one can tune the gap modes to the desired frequency. One can then detect IR radiation of the specified frequency by monitoring the film temperature.

We emphasize that these suggestions are quite speculative and that we mention them only because they deserve further contemplation and/or experimental testing.

Acknowledgement. We are grateful to National Science Foundation (CHE 79-18773) and the Office of Naval Research for partial support of this work.

References

- [1] For reviews see
- (a) R. VanDuyne, in *Chemical and Biochemical Applications of Lasers*, Vol. 4, Ed. C.B. Moore (Academic Press, New York, 1978).
 - (b) S. Efrima and H. Metiu, *Israel J. Chem.* 18, 17 (1979).
 - (c) E. Burstein, C.Y. Chen and S. Lundquist, in *Light Scattering in Solids*, ed. J.L. Birman, H.Z. Cummins and K.K. Rebane, Plenum Press, New York, 1979, p. 479.
 - (d) T.E. Furtak and J. Reyes, *Surface Sci.* 93, 351 (1980).
 - (e) A. Otto, *Proc. 6th Solid-Vacuum Interface Conference*, Delft, The Netherlands, May 7-9, 1980; *Applied Surface Sci.* 6, 308 (1980).
 - (f) R.K. Chang and T.F. Furtak, eds., *Surface Enhanced Raman Scattering*, Plenum, New York, 1981.
 - (g) H. Metiu, *Prog. Surface Sci.* (submitted).
- [2] S. Efrima and H. Metiu, *J. Chem. Phys.* 70, 1939 (1979); *ibid* 70, 1602 (1979); *ibid* 20, 2297 (1979).
- [3] (a) Y.J. Chen, W.P. Chen and E. Burstein, *Phys. Rev. Lett.* 36, 1207 (1976); W.P. Chen, G. Ritchie and E. Burstein, *Phys. Rev. Lett.* 37, 993 (1976).
- (b) For reviews see M.R. Philpott, in "Topics in Surface Chemistry," E. Kay and P.S. Bagus, eds., Plenum, New York 1979, p. 329; A. Otto in "Optical Properties of Solids - New Developments" B.O. Seraphin ed. North-Holland, Amsterdam (1976) p. 677.
 - (c) For application to surface enhanced Raman see B. Pettinger, A. Tadjeddine and D.M. Kolb, *Chem. Phys. Lett.* 66, 544 (1979); R. Dornhaus, R.E. Benner, R.K. Chang and I. Chabay, *Surface Sci.* 101, 367 (1980).

- (d) For applications to fluorescence see W.H. Weber and C.F. Eagen, *Optics Letters*, 4, 236 (1979); R.E. Benner, R. Dornhaus and R.K. Chang, *Optics Commun.* 30, 145 (1979); C.F. Eagen, W.H. Weber, S.L. McCarthy and R.W. Terhune, *Chem. Phys. Lett.* 75, 274 (1980); I. Pockrand, A. Brillante and D. Mobius, *Nuovo Cimento*, 63B, 350 (1981).
- [4] (a) Theory: S.S. Jha, J.R. Kirtley and J.C. Tsang, *Phys. Rev.* B22, 3973 (1980); P.K. Aravind, E. Hood and H. Metiu, *Surface Sci.* 109, 95 (1981).
- (b) Experiments: J.C. Tsang, J.R. Kirtley and J.A. Bradley, *Phys. Rev. Lett.* 43, 772 (1979); A. Girlando, M.R. Philpot, D. Heitman, J.D. Swalen and R. Santo, *J. Chem. Phys.* 72, 5187 (1980); P.N. Sanda, J.M. Warlaumont, J.E. Demuth, J.C. Tsang, K. Christmann and J.A. Bradley, *Phys. Rev. Lett.* 45, 1519 (1980); A. Adams, J. Moreland and P.K. Hansma, *Surface Sci.* 111, 351 (1981); A. Adams, J. Moreland, P.K. Hansma, L. Schlesinger, *Phys. Rev. B* (submitted).
- [5] (a) Theory: S.L. McCall, P.M. Platzman and P.A. Wolff, *Phys. Lett.* 77A, 381 (1980); J.I. Gersten, *J. Chem. Phys.* 72, 5779, 5780 (1980); J.I. Gersten and A. Nitzan, *J. Chem. Phys.* 73, 3023 (1980); D.-S. Wang, H. Chew and M. Kerker, *Appl. Opt.* 19, 2256 (1980); M. Kerker, D.-S. Wang and H. Chew, *Appl. Opt.* 19, 3373 (1980); F.J. Adrian, *Chem. Phys. Lett.* 78, 45 (1981); D.-S. Wang and M. Kerker, *Phys. Rev.* B24, 1777 (1981); B.J. Messinger, K. Ulrich von Raben, R.K. Chang and P.W. Barber, *Phys. Rev.* B24, 649 (1981).

- (b) Experiments with colloids: J.A. Creighton, C.G. Blatchford and M.G. Albrecht, *J. Chem. Soc., Faraday Trans. II*, 75, 790 (1979); M. Kerker, O. Siiman, L.A. Bumm and D.-S. Wang, *Appl. Optics*, 19, 3253 (1980); H. Wetzol and H. Gerischer, *Chem. Phys. Lett.* 76, 460 (1980); K.U. von Raben, R.K. Chang and B.L. Laube, *Chem. Phys. Lett.* 79, 465 (1981).
- (c) Experiments with islands: C.Y. Chen and E. Burstein, *Phys. Rev. Lett.* 45, 1287 (1980); E. Burstein, C.Y. Chen and S. Lundquist, *Proc. US-USSR Symposium on Inelastic Light Scattering from Solids*, eds. J.L. Birman, H.Z. Cummins and K.K. Rebane, (Plenum, 1979), p. 479; E. Burstein and C.Y. Chen, *Proc. CII-th International Conference on Raman Spectroscopy*, ed. W.F. Murphy (North Holland, 1980), p. 346; P.F. Liao, J.G. Bergman, D.S. Chemla, A. Wokaum, J. Melngailis, A.M. Hawryluk and N.P. Economu, *Chem. Phys. Lett.* 82, 355 (1981); J.C. Bergman, D.S. Chemla, P.F. Liao, A.M. Glass, A. Pinczuk, R.M. Hart and D.H. Olson, *Optics Lett.* 6, 33 (1980); D.A. Weitz, S. Garoff and T.J. Gramilla, *Optics Lett.* (submitted); J.G. Bergman, D.S. Chemla, P.F. Liao, A.M. Glass, A. Pinczuk, R.M. Hart and D.H. Olson, *Optics Lett.* 6, 33 (1981); A.M. Glass, P.F. Liao, J.G. Bergman and D.H. Olson, *Optics Lett.* 5, 368 (1980); S. Garoff, D.A. Weitz, T.J. Gramila and C.D. Hanson, *Optics Lett.* 6, 245 (1981); D.A. Weitz, S. Garoff, C.D. Hanson, T.J. Gramila and J.I. Gersten, *Optics Lett.* (submitted).
- [6] P.K. Aravind, A. Nitzan and H. Metiu, *Surface Sci.* 110, 189 (1981).

- [7] (a) Theory: P.K. Aravind and H. Metiu, Chem. Phys. Lett. 74, 301 (1980); J. Arias, P.K. Aravind and H. Metiu, Chem. Phys. Lett. (in press).
- (b) Experiments: G.L. Eesley, Phys. Rev. B24, 5477 (1981).
- [8] (a) There is a large body of electrochemical literature that has not been reviewed recently. For reviews see Ref. 1(a), (b), (d) and (e).
- (b) For UHV work see: J.E. Rowe, C.V. Shank, D.A. Zwemer and C.A. Murray, Phys. Rev. Lett. 44, 1770 (1980); T.H. Wood, D.A. Zwemer, C.V. Shank and J.E. Rowe, The Dependence of Surface Enhanced Raman Scattering on Surface Preparation: Evidence for an Electromagnetic Mechanism (preprint, 1981); R.R. Smardewski, R.J. Coulton and J.S. Murday, Chem. Phys. Letters, 68, 53 (1979); T.H. Wood and M.V. Klein, Solid State Commun. 35, 263 (1980); T.H. Wood, M.V. Kline and D.A. Zwemer, Surface Sci. 107, 625 (1981); G.L. Eesley, Phys. Letters 81A, 193 (1981); G.L. Eesley and J.M. Burkstrand, Phys. Rev. B24, 582 (1981); H. Seki and M.R. Philpott, J. Chem. Phys. 73, 5376 (1980); H. Seki, J. Vac. Sci. Tech. 18, 633 (1981); H. Seki, Surface Sci. (accepted); H. Seki, The role of direct surface interaction in surface enhanced Raman scattering by pyridine and CO on silver (preprint); I. Pockrand and A. Otto, Solid State Commun. 38, 1159 (1981); I. Pockrand and A. Otto, Solid State Commun. 37, 109 (1981); I. Pockrand and A. Otto, Appl. Surface Sci. 6, 362 (1980).

- [9] H. Abe, K. Manzel, W. Schultze, M. Moskovits and D.P. LiLella, J. Chem. Phys, 74, 792 (1981).
- [10] R.R. Chance, A. Prock and R. Silbey, in Advances in Chemical Physics, ed. I. Prigogine and S.A. Rice (Wiley, N.Y. 1978) p. 1-65.
- [11] P.M. Morse and H. Feshbach, Methods of Theoretical Physics (McGraw-Hill, New York, 1953) p. 1298.
- [12] J.A. Stratton, Electromagnetic Theory (McGraw-Hill, New York, 1941), p. 570.
- [13] Ref. 12, p. 492-494.
- [14] N.W. Ashcroft and N.D. Mermin, Solid State Physics, (Holt, Rinehart and Winston, 1976).
- [15] P.K. Aravind, R.W. Rendell and H. Metiu, Chem. Phys. Lett. 85, 396 (1982).
- [16] H.J. Hagemann, W. Gudat and C. Kunz, DESY Report No. SR-74/7 (May, 1974).
- [17] W.G. Spitzer, D.A. Kleinmann and C.J. Frosch, Phys. Rev. 113, 133 (1959).
- [18] A.S. Barker, Surface Sci. 34, 62 (1973).
- [19] I. Pockrand, J.D. Swalen, J.G. Gordon II and M.R. Philpott, J. Chem. Phys. 70, 3401 (1979).
- [20] H. Metiu, The use of reciprocity theorem in surface enhanced spectroscopy, unpublished.

Figure captions

Fig. 1. The geometry of the system: A planar interface separates the active medium, characterized by a complex frequency-dependent dielectric constant $\epsilon_1(\omega)$, from an "inert" medium of dielectric constant ϵ_0 . Imbedded in the inert medium at distance D above the interface is a perfectly conducting spherical particle of radius R_0 . The incoming laser beam has a wavevector \vec{k} and electric field \vec{E}_0 . The figure shows a p-polarized beam.

Fig. 2. Resonance spectrum of a Ag substrate with a perfectly conducting sphere on it. The intensity enhancement ratio \tilde{I} (defined in text) has been plotted as a function of the incident laser frequency in eV. The laser beam is incident at angle $\theta_0 = 45^\circ$ and is p-polarized. The full line is computed for $\lambda = 0.05$ (e.g., $R_0 \approx 100 \text{ \AA}$, $D = 5 \text{ \AA}$); the dotted line is for $\lambda = 0.1$ (e.g., $R_0 \approx 100 \text{ \AA}$, $D = 10 \text{ \AA}$). The value of FA indicated for each curve is the factor by which the vertical axis must be multiplied to obtain the value of \tilde{I} for that curve. This convention is followed on all subsequent figures.

Fig. 3a. Same as Fig. 2, but the substrate is β -SiC

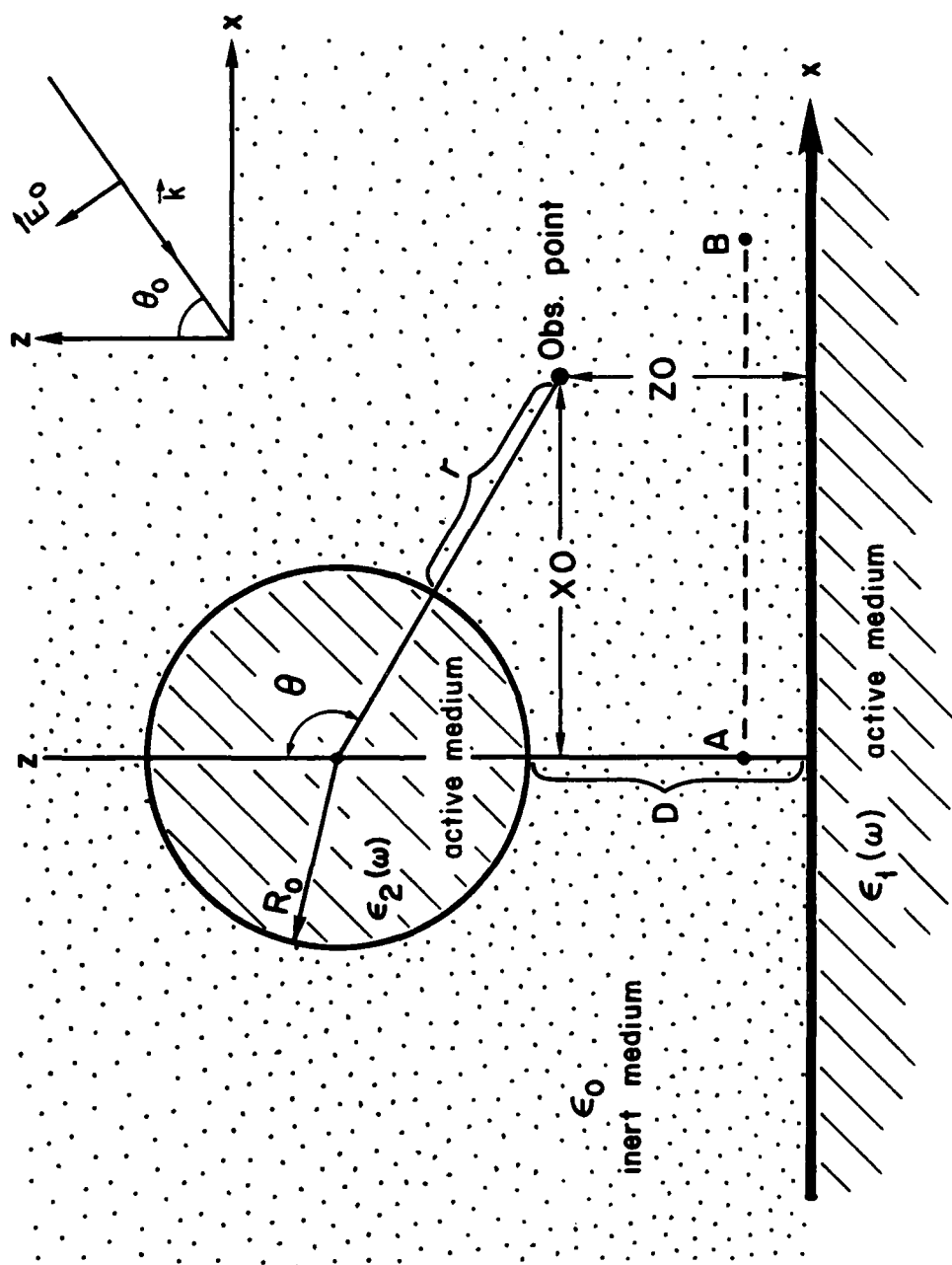
Fig. 3b. Same as Fig. 2, but the substrate is β -SiC and the incident light is s-polarized.

- Fig. 4a. Same as Fig. 2, but the substrate is n-type InSb; the substrate is lightly doped and has a free electron concentration corresponding to a plasma frequency of $\omega_p = 195 \text{ cm}^{-1}$.
- Fig. 4b. Same as Fig. 4a, but with a heavily doped substrate corresponding to $\omega_p = 1023 \text{ cm}^{-1}$.
- Fig. 5. Same as Fig. 2, but with an organic substrate.
- Fig. 6. The plot of $\text{Im}X(\omega)$ and $\text{Re}X(\omega)$ for a SiC substrate for $\lambda = 0.05$. The horizontal lines represent $\exp[(2n+1)\mu_0]$ for $n=0, 1, 2, 3$. See Section III.4 for a further discussion.
- Fig. 7. Spatial variation of enhancement ratio \tilde{I} at resonance. $\text{Log}_{10} \tilde{I}$ is plotted as a function of the angular coordinate θ for fixed $r = 1 \text{ \AA}$. The full line is for a Ag substrate and $\omega = 3.27 \text{ eV}$; the ~~dotted~~ dash-dot line is for a SiC substrate, $\omega = 916 \text{ cm}^{-1}$. The system parameters are $\lambda = 0.05$ (e.g., $R_0 = 100 \text{ \AA}$, $D = 5 \text{ \AA}$). The external laser is incident at $\theta_0 = 60^\circ$ and is p-polarized.
- Fig. 8. Same as Fig. 7 but with the following substrates: dotted line for a n-type InSb ($\omega_p = 1023 \text{ cm}^{-1}$), and $\omega = 931 \text{ cm}^{-1}$; the dashed line is for an organic material substrate and $\omega = 2.27 \text{ eV}$.
- Fig. 9. $\text{Log}_{10} \tilde{I}$ plotted as a function of the coordinate ZO for $XO = 0$ (along z-axis). The system parameters and substrates used are identical to those in Figs. 7 and 8.
- Fig. 10. $\text{Log}_{10} \tilde{I}$ plotted as a function of the co-ordinate XO for $ZO = 1 \text{ \AA}$. The system parameters and substrates used are identical to those in Figs. 7 and 8.

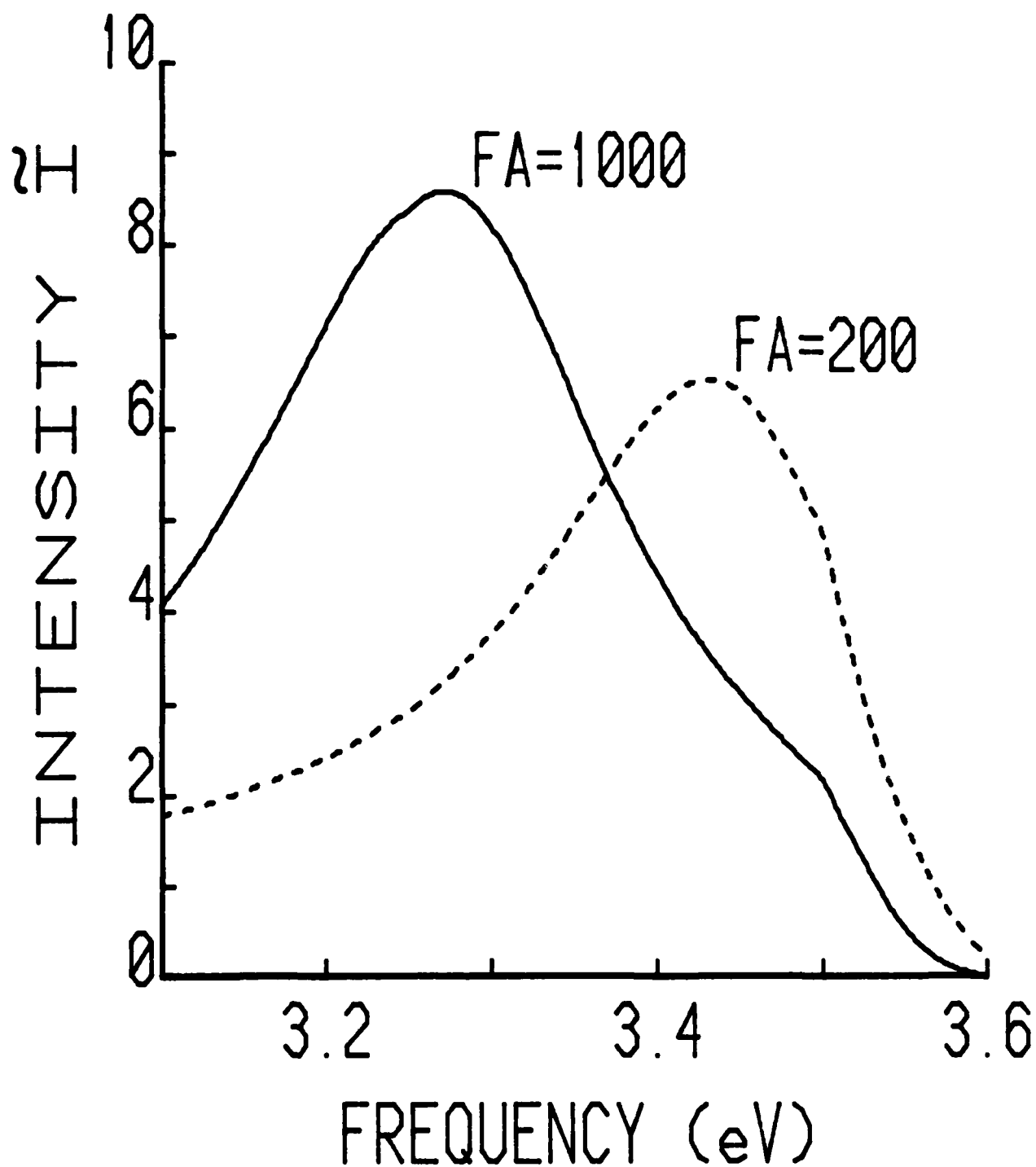
Table 1.

An analysis of the contributions of the gap modes
to the frequency dependence of the local intensity.
See Section III.4 for discussion.

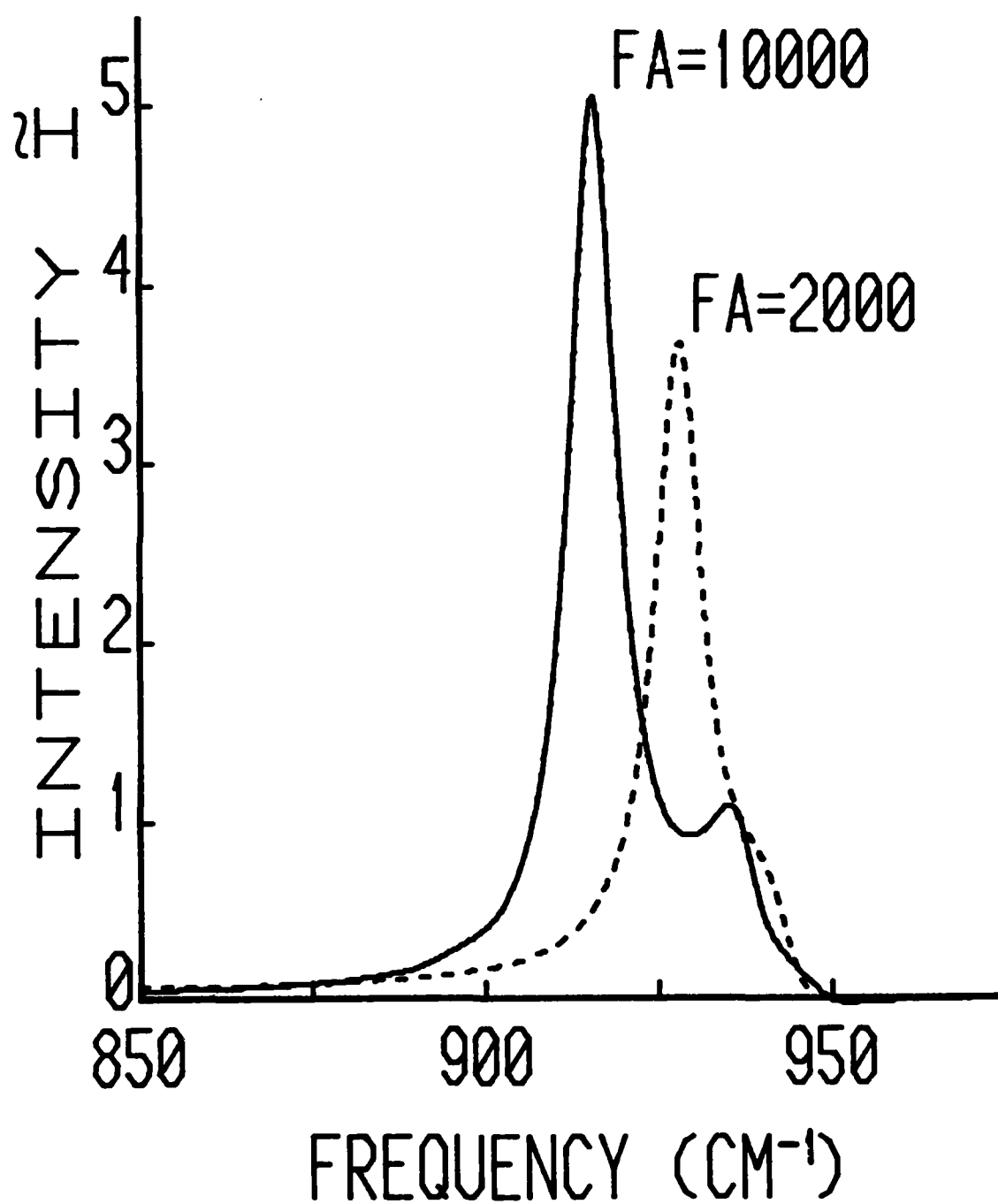
n	$ A_n^o $	$e^{(n+1/2)\mu_0}$	$e^{(n+1/2)\mu_0} A_n^o $
0	938.64	1.17	1098.71
1	180.24	1.60	289.07
2	98.21	2.20	215.82
3	56.20	3.01	169.22
4	32.57	4.13	134.35
5	18.87	5.65	106.65
6	10.88	7.74	84.23
7	6.23	10.61	66.08
8	3.54	14.54	51.50



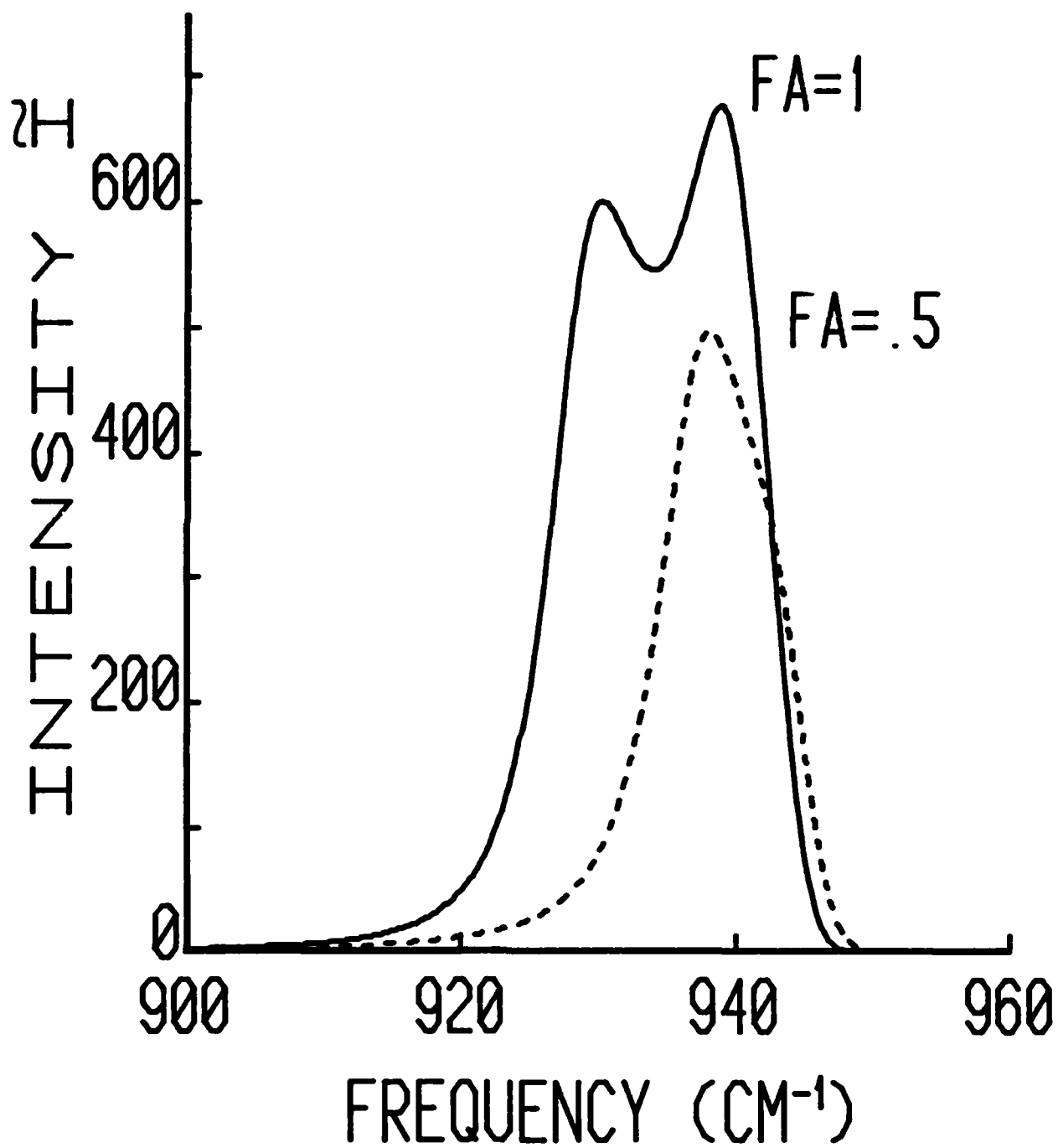
Ag SUBSTRATE



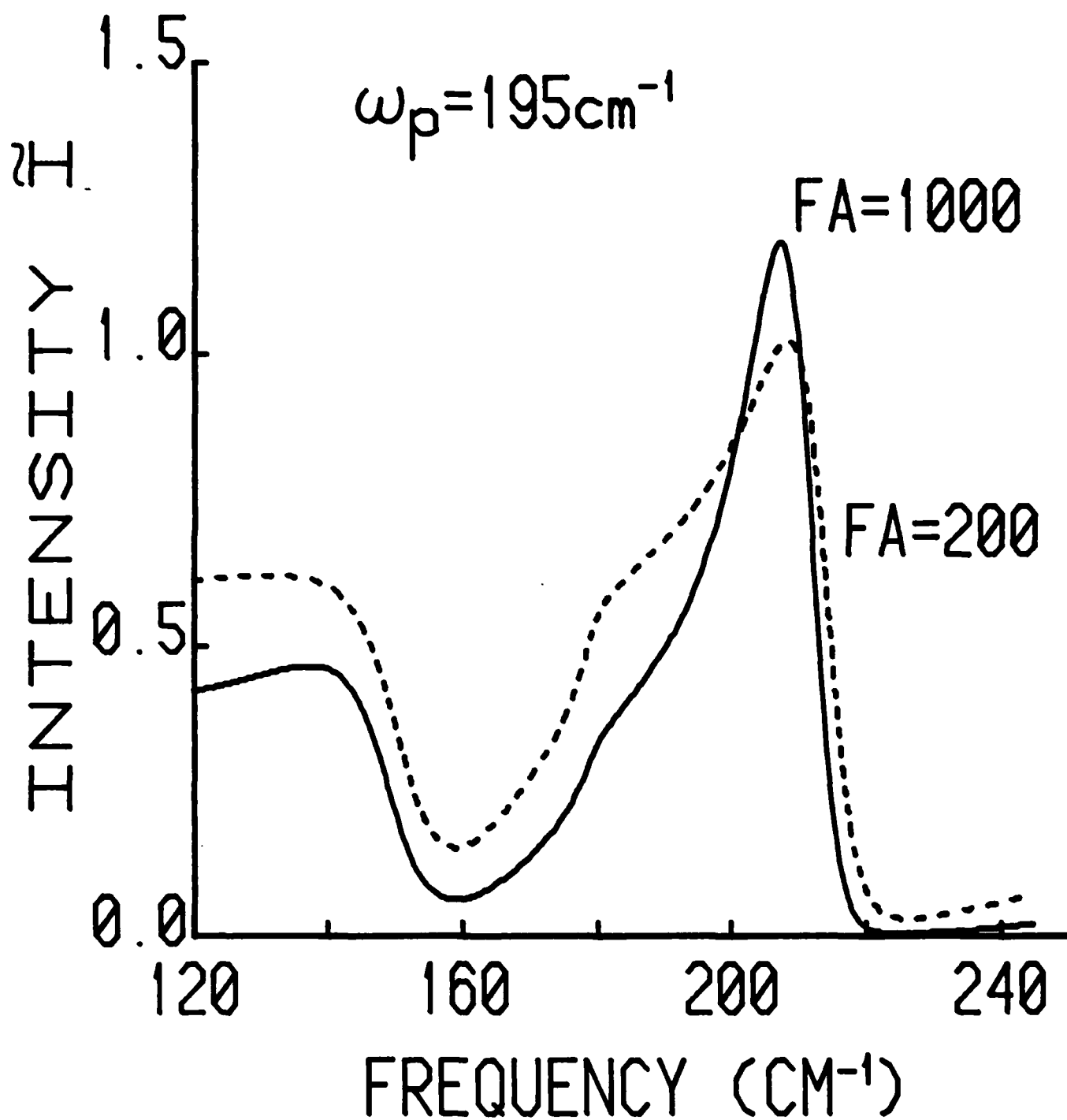
SiC SUBSTRATE



SiC SUBSTRATE

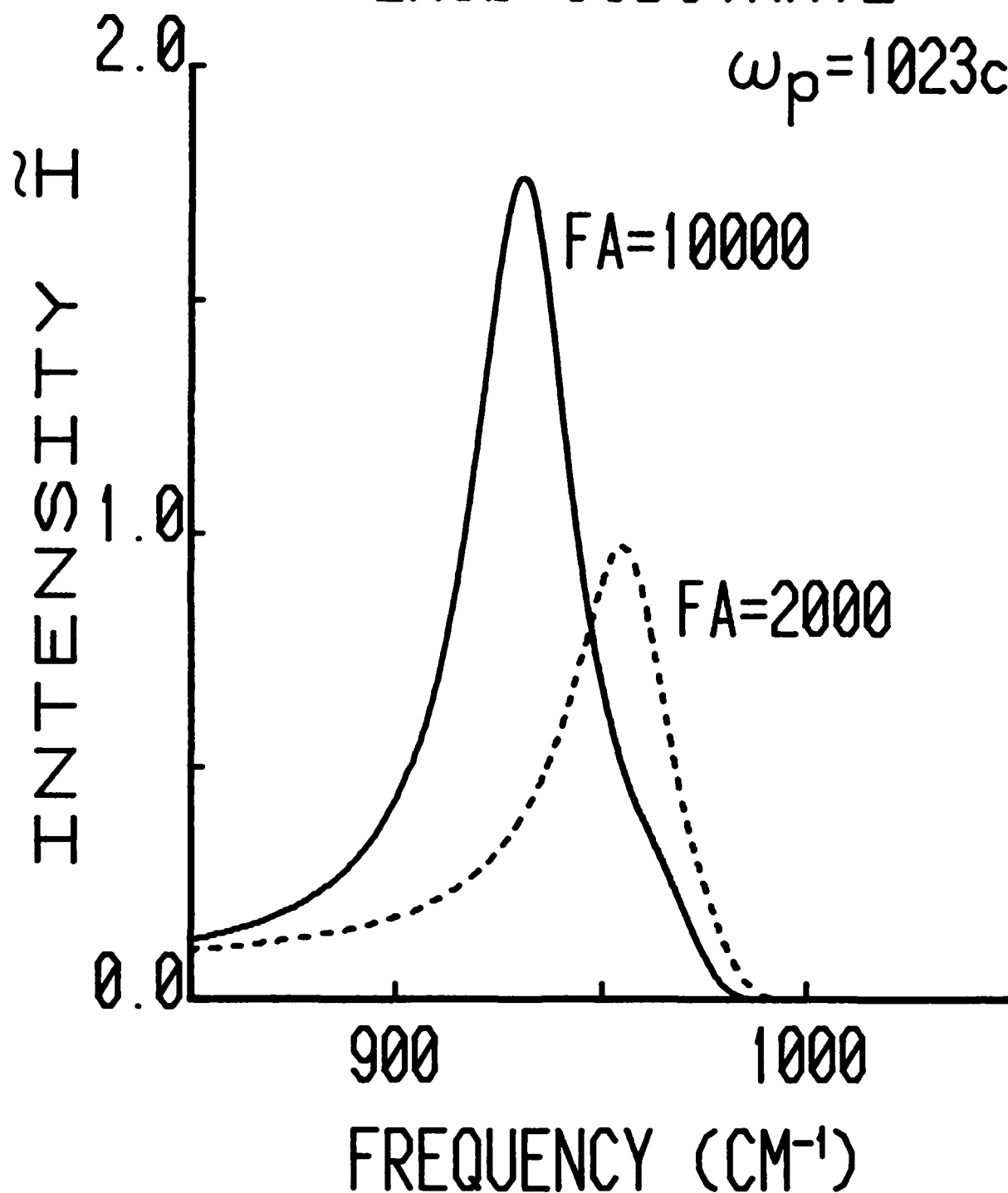


InSb SUBSTRATE



InSb SUBSTRATE

$$\omega_p = 1023 \text{ cm}^{-1}$$



ORGANIC SUBSTRATE

